

## Measurement of $^1\text{H}$ - $^1\text{H}$ Coupling Constants in DNA Fragments by 2D NMR

AD BAX AND LAURA LERNER

*Laboratory of Chemical Physics, National Institute of Diabetes and Digestive and Kidney Diseases, National Institutes of Health, Bethesda, Maryland 20892*

Received October 19, 1987; revised January 5, 1988

It is shown that a modified version of the recently proposed P.E.COSY experiment is ideally suited for measuring couplings to the H2' and H2'' protons in DNA. These couplings uniquely determine the phase of the pseudorotation of the deoxyribose ring. In addition, the coupling between H3' and H4' can be measured from a cross section through the H3'-H4' cross peak in a COSY spectrum that incorporates  $F_1$  decoupling of the H3' interaction with the H2'/H2'' protons. Simple guidelines are presented that permit estimating the accuracy of couplings measured from partially resolved antiphase doublets, as encountered for the H3'-H4' cross peaks. The experiments are demonstrated for the dodecamer d(CGCGAATTCGCG)<sub>2</sub>. © 1988 Academic Press, Inc.

### INTRODUCTION

In recent years, many reports have appeared concerning determination of the three-dimensional structure of DNA oligomers by means of 2D NMR (1-4). These studies have relied almost exclusively on a quantitative or semiquantitative interpretation of NOE buildup rates. Because significant changes in the conformation of the deoxyribose are possible without affecting the NOEs between sugar protons very much, it is difficult to obtain detailed information regarding the conformation of the deoxyribose sugars from NOEs. In principle, this information can be obtained from the homonuclear proton-proton coupling constants between the various sugar protons. Optimized Karplus equations for deoxyribose, corrected for the electronegativity of substituents and for the Barfield effect for cis couplings (5), have been developed and applied by Altona and co-workers (6, 7). In practice, these couplings are often not resolvable for DNA fragments of more than about five base pairs. This paper demonstrates the use of some simple methods for measuring the homonuclear coupling constants in larger DNA fragments. Couplings to the nonequivalent H2' and H2'' protons can be measured with the E.COSY experiment (8), or, as demonstrated here, with a shortened version of the recently proposed P.E.COSY experiment (9). The size of the coupling between H3' and H4' cannot be measured using this procedure. As shown here, an estimate for the size of this typically small coupling constant can be obtained from a modified COSY experiment where the couplings between H3' and the H2'/H2'' protons and  $^{31}\text{P}$  are removed in the  $F_1$  dimension of the 2D spectrum.

## FAST P.E.COSY

Mueller (9) recently proposed a simple method for recording 2D absorption-mode COSY spectra. He demonstrated that if his procedure is utilized in the COSY experiment with a small flip angle ( $<45^\circ$ ) for the mixing pulse, spectra very similar to E.COSY spectra can be obtained. In this so-called P.E.COSY experiment, a 2D matrix recorded without the mixing pulse present is subtracted from a matrix recorded with the small flip-angle mixing pulse. The residual diagonal signal in the difference spectrum thus loses its dispersive character when cross peaks are phased to be purely absorptive. Rather than recording an entire 2D matrix without a mixing pulse, we propose to use a single FID to generate this 2D reference spectrum.

An artificial 2D spectrum can be generated from a single FID, recorded with a data acquisition time twice as long as that used in the real 2D experiment; i.e., if  $N$  data points per  $t_1$  value are acquired in the real 2D experiment,  $2N$  data points are acquired for the single FID. Data for successive  $t_1$  values in the artificial matrix are then obtained by left shifting the data of the FID by one point for every  $t_1$  increment. After this left shift operation, only the first  $N$  data points are stored in the artificial 2D data matrix. To ensure that the artificial 2D data set has the correct intensity, the delay time between  $90^\circ$  pulses in the single FID experiment (which includes the data acquisition time) is chosen to be identical to the delay time between the  $90^\circ$  pulses in the real experiment with  $t_1 = 0$ .

To maximize the sensitivity in the final P.E.COSY spectrum, this single FID is recorded with about 16 times the number of scans used per  $t_1$  value in the real 2D experiment. Hence, when the artificial spectrum is scaled to the same absolute inten-

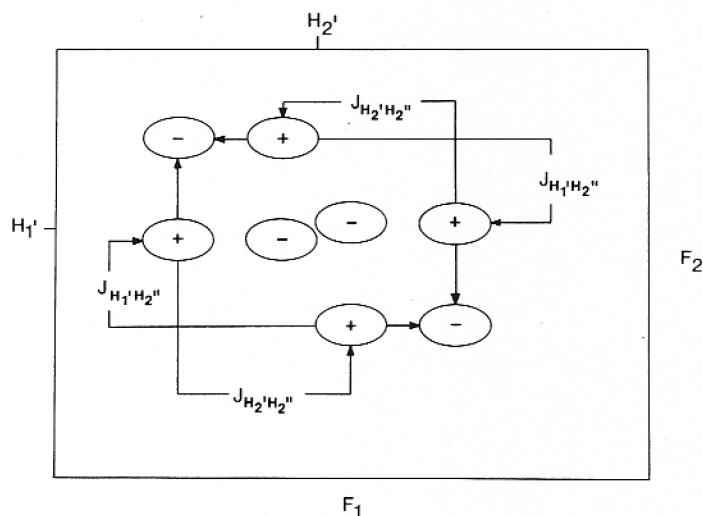


FIG. 1. Schematic diagram of a  $H_1'-H_2'$  cross multiplet in a P.E.COSY (or E.COSY) spectrum. The passive couplings,  $J_{1'2''}$  and  $J_{2'2''}$ , can be measured from such a cross peak as indicated in the figure. The arrows indicate the multiplet components to be used for measurement of the  $J$  coupling. The difference in linewidth commonly observed between the  $F_1$  and  $F_2$  dimensions is indicated by the ellipsoidal shape of the multiplet components.

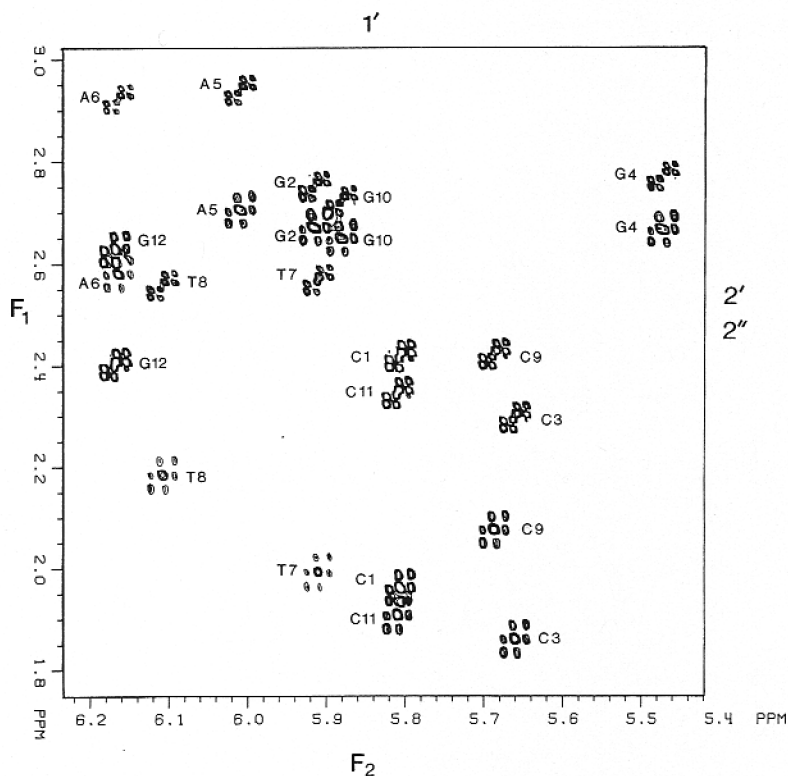


FIG. 2. H1'-H2', H2'' cross-peak region of the P.E.COSY spectrum of d(CGCGAATTCGCG)<sub>2</sub>. The spectrum results from a  $2 \times 512 \times 2048$  data matrix with acquisition times of 152 and 304 ms in the  $t_1$  and  $t_2$  dimensions. Digital resolution in the displayed spectrum is 1.6 and 0.8 Hz in the  $F_1$  and  $F_2$  dimensions, respectively. Chemical shifts for all 2'' protons are downfield from shifts for 2' protons, except for G12.

sity as the real COSY spectrum, the noise level in the artificial spectrum is four times lower. Subtracting the artificial spectrum from the real spectrum then increases the noise level in the difference spectrum by only 3%.

#### APPLICATION TO d(CGCGAATTCGCG)<sub>2</sub>

The E.COSY and P.E.COSY (if recorded with a small flip angle, typically  $36^\circ$ ) experiments are ideal for measuring couplings to nonequivalent methylene protons because only directly connected transitions contribute to the cross-peak multiplets. For deoxyribose this means, for example, that the H1'-H2' cross peak consists of two parts, corresponding to the  $\alpha$  and  $\beta$  spin states of the H2'' proton. Because the geminal H2'-H2'' coupling is quite large (about 14 Hz), these two parts can be resolved. Their relative displacements in the two frequency dimensions correspond to  $J_{2'-2''}$  and  $J_{1'-2''}$  (Fig. 1). Even if the natural linewidth is larger than the coupling constant (but not larger than the geminal coupling) accurate couplings can be measured from such a spectrum.

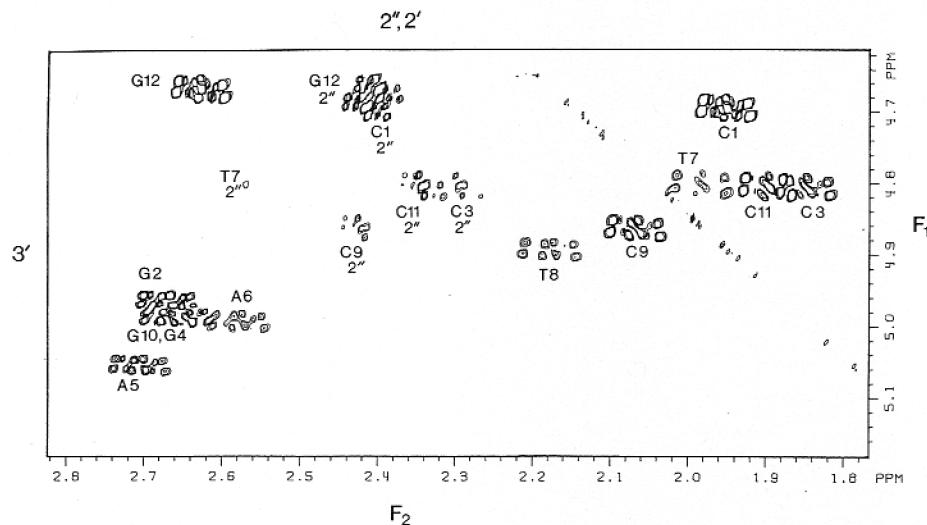


FIG. 3. H2', H2''-H3' cross-peak region of the spectrum. All parameters are identical to those of the spectrum of Fig. 2. Cross peaks correspond to H2'-H3' couplings unless otherwise labeled.

Figures 2 and 3 show the cross peaks between the H1' and H2'/H2'' protons and between the H2'/H2'' and the H3' protons, respectively. All H1'-H2'/H2'' couplings could be measured from the spectrum of Fig. 2. Unfortunately, the H2''-H3' coupling is small (1-2 Hz) in B DNA with a C2'-endo ring pucker (10). Therefore, this cross peak has a low intensity, making reliable measurement of the larger passive H2'-H3'

TABLE I

Homonuclear Proton Couplings to the H2' and H2'' Protons  
in d(CGCGAATTCGCG)<sub>2</sub>

Base	$J_{12}^a$	$J_{12}^b$	$J_{23}^c$	$J_{23}^c$
C1	8.2	6.1	6.3	2.8
G2	10.1	5.7		1.5
C3	8.8	6.2	6.1	2.3
G4	10.2	5.1		<2.0
A5	9.7	5.7		1.5
A6	9.3	6.0		1.5
T7	8.5	6.2		2.2
T8	9.5	6.0		1.6
C9	8.7	6.0	6.3	2.8
G10	9.7	5.5		<2.0
C11	8.4	6.2	6.6	2.6
G12	8.1	6.3	6.3	3.6

<sup>a,b,c</sup> Average standard deviations obtained by comparing four values measured from two separate experiments, averaged over all 12 nucleotides, are 0.12, 0.13, and 0.21 Hz, respectively.

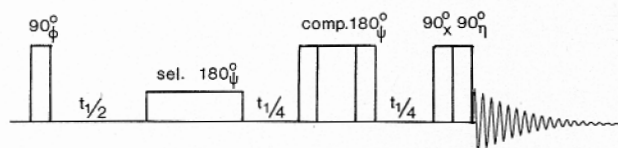


FIG. 4. Pulse scheme for the partially decoupled  $J$ -scaled double-quantum-filtered COSY spectrum. Phase cycling used is

$$\phi = x, y, -x, -y, x, y, -x, -y, x, y, -x, -y, x, y, -x, -y;$$

$$\psi = x, x, x, x, y, y, y, y, -x, -x, -x, -x, -y, -y, -y, -y;$$

$$\text{Receiver: } x, x, -x, -x, x, x, -x, -x, x, x, -x, -x, x, x, -x, -x.$$

After every 16 scans, the phase  $\eta$  is incremented by  $90^\circ$  and the receiver reference phase is decremented by  $90^\circ$ .

coupling very difficult. As indicated in Fig. 1, two independent measurements of the passive coupling can be made from a single cross peak. For practical reasons, digitization in the  $F_2$  dimension typically is much higher than in the  $F_1$  dimension and only one of the two cross peaks can be used for measuring the size of the passive coupling. The measured couplings are presented in Table 1. These  $J$  values represent the average value of couplings, measured in two separate experiments; i.e., for the nonoverlapping cross peaks the given value corresponds to the average of four measurements. As has been demonstrated previously (8), accurate couplings can be determined with the E.COSY experiment even if the coupling is much smaller than the natural linewidth. This approach for measuring passive couplings is virtually free of systematic errors, provided that the second passive coupling (in this case the  $H_2'/H_2''$  coupling) is larger than the linewidth. The reproducibility of the measured  $J$  values in the two experiments was excellent for the  $H_1'-H_2'/H_2''$  couplings with an average rms error of 0.12 Hz. The reproducibility for the  $H_2'/H_2''-H_3'$  couplings was not as good (0.21 Hz), mainly because of the lower signal-to-noise ratio and the partial overlap in this region of the P.E.COSY spectrum.

#### PARTIALLY DECOUPLED $J$ -SCALED DOUBLE-QUANTUM-FILTERED COSY

Because  $H_3'$  and  $H_4'$  do not share a common coupling partner, an approach differing from that described above is needed. Here we propose to measure the coupling between these two protons using the antiphase  $F_1$  doublet in a double-quantum-filtered (11)  $J$ -scaled (12) COSY experiment where the  $H_2'/H_2''$  and  $^3\text{P}$  couplings to  $H_3'$  are suppressed. The pulse scheme is sketched in Fig. 4. The soft pulse in the center of the evolution period is adjusted to be near  $180^\circ$  in the  $H_3'/H_4'$  region of the spectrum (centered at 4.6 ppm) and to have near-zero excitation in the  $H_2'/H_2''$  region of the spectrum (center at 2.5 ppm). At a proton frequency of 500 MHz, a rectangular  $180^\circ$  pulse of 1 ms duration is suitable for this purpose. The nonselective  $180^\circ$  pulse at the center of the second half of the evolution period suppresses chemical-shift evolution during this time, effectively scaling the range of frequencies that must be covered in the  $F_1$  dimension and decreasing the decay caused by field inhomogeneity in the  $t_1$  dimension by a factor of 2. To eliminate artifacts arising from

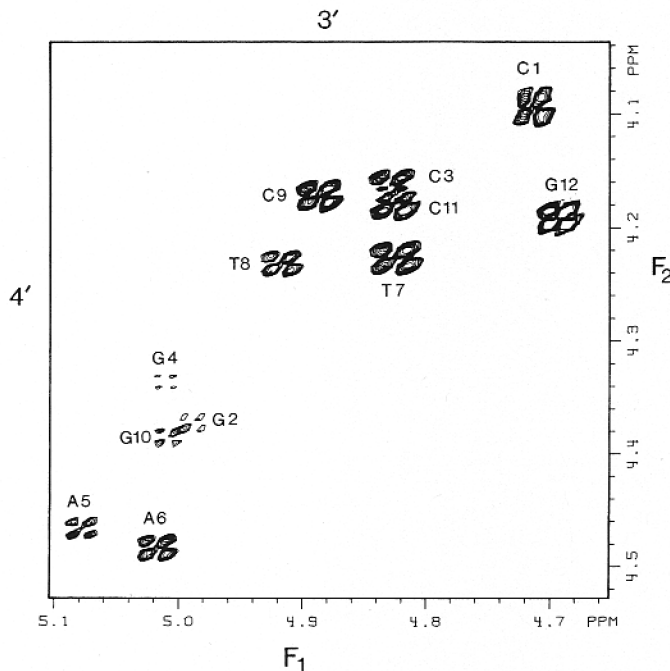


FIG. 5. H3'-H4' cross-peak region of  $d(\text{CGCGAATTCGCG})_2$  of the COSY spectrum recorded with the scheme of Fig. 4.  $J$  scaling by a factor of 2 was used; i.e., all  $J$  splittings are enlarged by a factor 2 in the  $F_1$  dimension. Digital resolution is 0.5 and 1.5 Hz in the  $F_1$  and  $F_2$  dimensions, respectively.

imperfect  $180^\circ$  pulses, both the soft  $180^\circ$  pulse and the nonselective  $180^\circ$  pulse would have to be phase cycled independently in the EXORCYCLE fashion (13). However, to minimize the number of phase-cycling steps needed per  $t_1$  value, the nonselective  $180^\circ$  pulse is a composite  $90^\circ_x 180^\circ_y 90^\circ_x$  (14) and the EXORCYCLE phase cycling is combined for the two pulses (see the legend to Fig. 2).

Figure 5 presents the H3'/H4' correlation region of the spectrum, using 1 Hz exponential line narrowing in the  $F_1$  dimension. The intensities of the 12 cross peaks vary significantly. In the  $F_1$  dimension only  $J_{3'4'}$  is observed; in the  $F_2$  dimension H4' is coupled to H3' (antiphase) and to H5'/H5'' (in-phase). The degree of cancellation of the antiphase multiplet structure in the  $F_2$  dimension depends not only on  $J_{3'4'}$  but also on  $J_{4'5'}$  and  $J_{4'5''}$ , resulting in the wide variation in cross-peak intensities visible in Fig. 5. In the  $F_1$  dimension some cancellation of cross-peak intensity also occurs, at least for the smallest  $J_{3'4'}$  couplings. As shown below, it is possible to determine whether the splitting measured from an antiphase doublet is close to the true value of the coupling or whether it represents an overestimate.

#### COUPLINGS FROM ANTIPHASE DOUBLETS

As is well known (15) and demonstrated in Fig. 6, the splitting measured for an unresolved antiphase doublet represents an overestimate of the actual coupling. In an attempt to obtain more accurate values for the coupling, one could try to fit the unresolved antiphase doublet to the difference of two equally intense resonances,

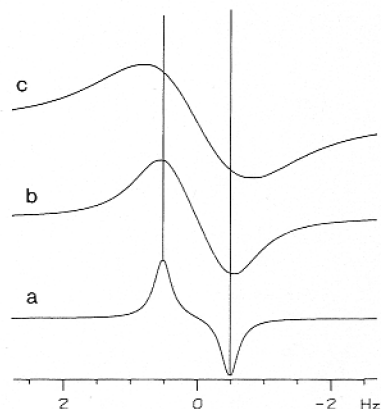


FIG. 6. Antiphase doublets with  $J = 1$  Hz and Lorentzian-shaped lines with halfwidths of (a) 0.3 Hz, (b) 1 Hz, and (c) 2 Hz.

displaced by an amount  $J$ . In practice, low signal-to-noise and the tedious nature of such an approach make this undesirable. It is demonstrated here that if the data are processed with different amounts of exponential multiplication, comparison of the measured splittings presents a simple method for determining whether the measured value is close to the true value or an overestimate. Figure 7a shows the measured splitting (maximum to minimum) of two antiphase Lorentzian lines that are 1 Hz apart, as a function of linewidth. As expected, for resonances with  $\Delta\nu_{1/2} < 1$  Hz, the splitting approaches the true coupling. For linewidths much larger than the coupling, the measured value increases linearly with linewidth. By determining the change in measured splitting as a function of linewidth ( $dS/d\Delta\nu_{1/2}$ ) it is possible to determine the severity of the overlap (Fig. 7b). Of course, the reliability of this procedure depends on the signal-to-noise ratio and also on the interpolation procedure used for determining the peak position and on the spectral digitization. The Nicolet software used in this study determines the peak position by Lorentzian interpolation of the three data points nearest to the extreme value. Tests on simulated antiphase doublet

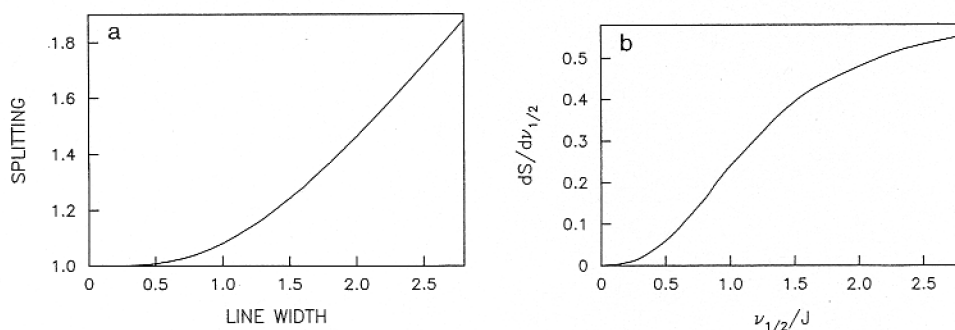


FIG. 7. (a) Peak to peak splitting measured for an antiphase doublet with a 1 Hz  $J$  coupling as a function of linewidth. (b) The relative change in measured splitting,  $S$ , as a function of the change in half-width to  $J$  coupling ratio,  $\nu_{1/2}/J$ .

signals to which random noise was added indicated that the length of the time-domain data had to be at least  $2T_2^*$ , where  $T_2^*$  indicates the decay constant after exponential multiplication in the  $t_1$  dimension. Zero-filling of the FID to four times its original length appeared to be adequate for reproducing the theoretical value of the splitting. At low signal-to-noise ratios ( $<10$ ) more zero-filling actually decreased the accuracy of the measured splitting. By determining the change in measured splitting as a function of the change in linewidth, the ratio  $J/\nu_{1/2}$  can be determined from Fig. 7b and an estimate for the true coupling then is obtained from Fig. 7a. The above discussion applies only to antiphase doublets; if passive couplings are also present, analysis of the antiphase splitting becomes much more complicated.

The scheme of Fig. 4 suppresses all passive couplings to H3' in the  $t_1$  dimension and therefore results in pure antiphase doublets in the  $F_1$  dimension of the 2D spectrum. The  $F_1$  splittings measured for three different amounts of line narrowing and the  $J_{3'4'}$  couplings derived from these data are presented in Table 2. Measured  $J_{3'4'}$  couplings show a direct correlation with cross-peak intensity. C1 is the only exception, with a relatively small coupling but an intense cross peak. This is probably due to increased mobility and consequently longer  $T_2$  values of this terminal nucleotide.

#### EXPERIMENTAL

All spectra were recorded on a Nicolet NT-500 spectrometer with a Cryomagnet Systems probe. Four hundred OD<sub>260</sub> units of d(CGCGAATTCGCG)<sub>2</sub> were dissolved in 0.5 ml D<sub>2</sub>O, p<sup>2</sup>H 7.3, 100 mM NaCl, 36°C. <sup>31</sup>P decoupling (0.1 W) with WALTZ modulation was used during evolution and detection periods.

The P.E.COSY spectrum resulted from a  $2 \times 512 \times 2048$  data matrix, correspond-

TABLE 2  
Measured Antiphase Splitting in the  $F_1$  Dimension  
of the H3'-H4' Cross Peaks in the  $J$ -Scaled  
Double-Quantum-Filtered Selective  
COSY Spectrum

Base	$\Delta_0^a$	$\Delta_{-1}^b$	$\Delta_{-2}^c$	$J_{3'4'}^d$
C1	3.59	3.42	3.35	3.3
G2	3.45	3.20	—	2.9
C3	4.30	3.93	3.60	3.4
G4	2.90	2.60	2.35	2.3
A5	3.16	2.83	2.63	2.5
A6	3.75	3.42	3.15	3.0
T7	5.08	4.88	4.77	4.7
T8	4.01	3.64	3.34	3.1
C9	4.14	3.88	3.66	3.6
G10	3.05	2.74	2.52	2.4
C11	4.40	4.19	4.08	4.0
G12	3.54	3.33	3.19	3.2

<sup>a,b,c</sup> Splittings measured with 0, 1, and 2 Hz exponential line narrowing, respectively.

<sup>d</sup> Coupling estimated from  $\Delta_{-0.5}$ ,  $\Delta_{-1}$ , and  $\Delta_{-1.5}$  values.

ing to data acquisition times of 152 and 304 ms in the  $t_1$  and  $t_2$  dimensions, respectively. Zero-filling was used in both dimensions to increase digital resolution. Sixty-four scans were acquired per  $t_1$  value, with a delay time of 2.2 s between scans, resulting in a total measuring time of 20 h. The 1D reference spectrum was acquired in a 4K data table, with 512 scans. Sample spinning was used to obtain the highest possible resolution. Spectral resolution was enhanced in both dimensions by digital filtering.

The  $J$ -scaled double-quantum-filtered spectrum resulted from a  $2 \times 256 \times 1024$  data matrix with acquisition times of 512 and 160 ms in the  $t_1$  and  $t_2$  dimensions, respectively. The transmitter was placed at 4.6 ppm and the duration of the soft  $180^\circ$  pulse was 1 ms. In the  $t_2$  dimension exponential line narrowing (6 Hz) and Gaussian line broadening (6 Hz) were used. In the  $t_1$  dimension exponential line narrowing (0,  $-1$  and,  $-2$  Hz) and zero-filling up to 2048 data points were used.

#### DISCUSSION

We have shown that most of the homonuclear couplings defining the deoxyribose pucker can be measured using the correlation techniques discussed above in a DNA fragment of 12 base pairs. The sugar puckers calculated from these couplings, using the PSEUROT program<sup>1</sup> developed by Altona and co-workers (6), are presented in Table 3. This program fits the data to an equilibrium of two rapidly interconverting conformers. In this program, the minor conformer is restricted to an  $N$ -type conformation with a phase angle of  $9^\circ$  and  $36^\circ$  amplitude of pucker. The conformations of the major conformers then are varied to give a best fit to the measured  $J$  couplings. The results are given in Table 3 and indicate that for all sugars very reasonable conformations were obtained for the major conformer.

The important remaining question is whether accurate measurements of  $J$  couplings contain information not available from careful NOE buildup studies; i.e., could a combination of  $J$  couplings and NOE distance information provide a better structure than an energy-minimized structure derived from NOE and other constraints alone? A detailed comparison of the structures generated from NOE data with and without the use of  $J$  coupling information is needed to evaluate the importance of  $J$  couplings for the DNA structure. Preliminary results of such a comparison indicate relatively small but significant differences between the two structures.

As demonstrated here, the P.E.COSY (and E.COSY) method is ideally suited for measuring couplings to nonequivalent methylene protons. This is of importance not only for determining conformation of DNA oligomers but also for determining amino acid side-chain orientation in proteins. Since for many amino acids the  $C_\beta$  protons are nonequivalent the same procedure as that demonstrated here for DNA can be used for measuring the couplings between the  $C_\alpha$  and  $C_\beta$  protons. Similarly, the double-quantum-filtered  $J$ -scaled COSY experiment can be used for measuring NH- $C_\alpha$ H couplings, providing information about the peptide backbone, utilizing the relatively long  $T_2$  of the  $C_\alpha$  protons. Because measured  $J$  couplings reflect the time average of the actual couplings, measurement of couplings provides important addi-

<sup>1</sup> The PSEUROT program was obtained from the QCPE program exchange. The program was modified such that weighting factors could be added to each of the measured couplings, reflecting the difference in accuracy of the various couplings. For the results of Table 3, we used weighting factors of 1 for  $J_{1'2'}$ , and  $J_{1'2''}$ , and 0.5 for all other measured couplings.

TABLE 3

Conformations of the *S*-Type Conformers of the Deoxyribose Sugars in d(CGCGAATTCGCG)<sub>2</sub>, Derived from the *J* Couplings of Tables 1 and 2<sup>a</sup>

Base	Phase	Amplitude	%S
C	151	35.2	78
G	136	35.8	97
C	150	34.5	84
G	144	38.0	99
A	146	35.0	94
A	141	32.9	93
T	124	34.2	85
T	137	32.9	95
C	144	36.5	80
G	148	36.3	93
C	140	34.8	79
G	157	34.9	74

<sup>a</sup> The conformation of the *N*-type conformer was restricted to a phase angle of 9° and 36° pucker amplitude.

tional information (not directly available from NOEs) on the average orientation of partially mobile molecular fragments.

#### ACKNOWLEDGMENTS

We thank Dr. Bernard Brooks for modifying the PSEUROT program and R. Tschudin for continuous technical support. L. Lerner is the recipient of an Arthritis Foundation postdoctoral fellowship.

#### REFERENCES

1. D. R. HARE, D. E. WEMMER, S. H. CHOU, G. DROBNY, AND B. R. REID, *J. Mol. Biol.* **171**, 319 (1983).
2. R. M. SCHEEK, N. RUSSO, R. BOELEN, R. KAPTEIN, AND J. H. VAN BOOM, *J. Am. Chem. Soc.* **105**, 2914 (1983).
3. J. FEIGON, W. A. DENNY, W. LEUPIN, AND D. R. KEARNS, *Biochemistry* **22**, 5930 (1983).
4. M. NILGES, G. M. CLORE, A. M. GRONENBORN, A. T. BRUNGER, M. KARPLUS, AND L. NILSSON, *Biochemistry* **26**, 3718 (1987).
5. J. L. MARSHALL, S. R. WALTER, M. BARFIELD, A. P. MARCHAND, N. W. MARCHAND, AND A. L. SEGRE, *Tetrahedron* **32**, 537 (1976).
6. F. A. A. M. DE LEEUW AND C. ALTONA, *J. Comput. Chem.* **4**, 428 (1983).
7. F. A. A. M. DE LEEUW AND C. ALTONA, *J. Chem. Soc., Perkin Trans. 2*, 375 (1982).
8. C. GRIESINGER, O. W. SØRENSEN, AND R. R. ERNST, *J. Am. Chem. Soc.* **107**, 6394 (1985).
9. L. MUELLER, *J. Magn. Reson.* **72**, 191 (1987).
10. D. B. DAVIES, *Prog. NMR Spectrosc.* **12**, 135 (1978).
11. U. PIANTINI, O. W. SØRENSEN, AND R. R. ERNST, *J. Am. Chem. Soc.* **104**, 6800 (1982).
12. B. T. FARMER II AND L. R. BROWN, *J. Magn. Reson.* **71**, 365 (1987).
13. G. BODENHAUSEN, R. FREEMAN, AND D. L. TURNER, *J. Magn. Reson.* **27**, 511 (1977).
14. M. H. LEVITT AND R. F. FREEMAN, *J. Magn. Reson.* **43**, 65 (1981).
15. D. NEUHAUS, G. WAGNER, M. VASAK, J. H. R. KAGI, AND K. WÜTHRICH, *Eur. J. Biochem.* **151**, 257 (1985).